RSC Advances

PAPER

View Article Online
View Journal | View Issue

Check for updates

Cite this: *RSC Adv.*, 2022, **12**, 32210

Ascorbic acid enhanced ferrous/persulfate system for degradation of tetracycline contaminated groundwater†

Hengyi Wang,[ab] Liyang Zhao,[ab] Qian Li,[ab] Xixiang Liu, *[abc] Liying Liang,[ab] Jianmei Cen,[ab] Yan Liu[ab] and Honghui Pan[ab]

Persulfate (PS) activated by Fe(II) has been widely investigated for degradation of contaminants. However, the Fe(II)/PS systems used for actual contaminated groundwater remediation have been restricted by circulation of Fe(III)/Fe(II). Herein, an ascorbic acid (AA) enhanced Fe(II)/PS system was developed for degradation of tetracycline (TC) contaminated groundwater. The influence of Fe(II), AA, PS dosage and pH on degradation of TC was investigated, the free radicals produced in the reaction were identified and the reusability of Fe(II) in the Fe(II)/PS/AA system for degradation of TC was also evaluated. The results showed that AA significantly promoted the degradation of TC in the Fe(II)/PS system, and a degradation rate of 86% for TC was achieved at 60 min. The dominant oxidant species for contaminant degradation in the Fe(II)/PS/AA system is $^{\bullet}OH$. Appropriate Fe(II), AA and PS dosage can improve the degradation rate of TC. Moreover, the degradation rate of TC in the Fe(II)/PS/AA system under acidic conditions is higher than that under alkaline conditions. With the increase of reaction time, TC can also be completely degraded even with a little Fe(II) or under alkaline conditions in the Fe(II)/PS/AA system, and Fe(II) showed a good reusability for the degradation of TC. Thus, the AA-enhanced Fe(II)/PS system for the degradation of contaminants displays the advantages of less Fe(II) consumption and a wide range of pH. This method provides a new strategy for *in situ* remediation of contaminated groundwater.

Received 27th July 2022
Accepted 24th October 2022

DOI: 10.1039/d2ra04694f

rsc.li/rsc-advances

Open Access Article. Published on 09 November 2022. Downloaded on 7/28/2025 11:05:35 AM.
This article is licensed under a Creative Commons Attribution-NonCommercial 3.0 Unported Licence.

1. Introduction

Due to the abuse of pharmaceutical antibiotics and the rapid expansion of animal husbandry and aquaculture, China has become a major country for the use of antibiotics. In 2013, the consumption of antibiotics in China was about 1.62×10^5 tons, accounting for about half of the global consumption.[1] The residual antibiotics eventually enter the natural environment. Recent studies have shown that in addition to surface water and soil,[2,3] antibiotics have also been detected in groundwater.[4–6] Although the concentration of antibiotics in groundwater is lower than that in surface water, it can be enriched through the food chain and seriously endangers human health. Therefore, it is of great significance to study the remediation methods of antibiotics-contaminated groundwater.

Sulfate radicals based advanced oxidation processes (AOPs) have many advantages, such as free radicals have a good oxidation performance and long half-life of oxidizing species after being activated, and easy to transport and store for the oxidants.[7] So, sulfate radicals ($SO_4^{\bullet-}$) based AOPs have been one of the research hotspots in contaminated groundwater remediation.[8–10] Generally, persulfate (PS) can be activated by means of light radiation,[11] heat,[12] alkaline,[13] carbon materials,[14,15] metal oxides[16] and transition metals,[17,18] and so on. Among the various activation methods, Fe(II) has been widely used as a activator for persulfate due to its reducibility, low cost and non-toxicity. At present, persulfate activated by Fe(II) for degradation of contaminants has been widely reported.[19–22] The Fe(II)/PS system has the advantages of short reaction time, simple operation and high efficiency. However, it has some drawbacks. Firstly, it is necessary to continuously add Fe(II) to fully degrade contaminants, because Fe(II) is difficult to be regenerated when it is oxidized to Fe(III). This might lead to the production of large amounts of iron sludge and cause secondary pollution on the environment. Secondly, the applicable pH range of this reaction is narrow.[23] Therefore, the Fe(II)/PS system used for actual contaminated groundwater remediation have been restricted.

To overcome these problems, improvements are mainly made in the following three aspects. Firstly, a chelating agent is

[a]*Guangxi Colleges and Universities Key Laboratory of Environmental-friendly Materials and New Technology for Carbon Neutralization, Guangxi Key Laboratory of Advanced Structural Materials and Carbon Neutralization, School of Materials and Environment, Guangxi Minzu University, Nanning 530006, China. E-mail: liuxx200208@163.com*

[b]*Research Center for Soil and Groundwater Environment, Guangxi Minzu University, Nanning 530006, China*

[c]*Guangxi Research Institute of Chemical Industry Co., Ltd., Nanning 530001, China*

† Electronic supplementary information (ESI) available. See DOI: https://doi.org/10.1039/d2ra04694f

© 2022 The Author(s). Published by the Royal Society of Chemistry

Open Access Article. Published on 09 November 2022. Downloaded on 7/28/2025 11:05:35 AM.
This article is licensed under a Creative Commons Attribution-NonCommercial 3.0 Unported Licence.

used to slowly release Fe(II) and then continuously activate PS.[24] Secondly, heterogeneous iron catalysts are employed to activate PS under wide pH range.[25] Thirdly, adding a lower dosage of Fe(II) to activate PS and some reductants are taken to promote Fe(II) regeneration. Among them, the method of promoting Fe(II) regeneration by adding reducing agents has attracted extensive attention because of its convenient and effective. It has been reported that reducing agent such as hydroxylamine is used to reduce Fe(III) to Fe(II) and effectively improve the sustainable ability of Fe(II) to activate PS.[26] Unfortunately, the above reducing agent and its degradation products are toxic, so we need to find an environment-friendly reducing agent.

Ascorbic acid (AA) is a natural reducing agent widely existing in nature. The oxidation–reduction process of contaminants caused by the coupling of AA and iron cycle is a common phenomenon in nature.[27–30] More recently, it has been reported that AA can promote the movement of Fe(III) to Fe(II) in Fenton reaction system and its degradation effect on organic contaminants.[31] To the best of our knowledge, there was little work on the use of AA in $SO_4^{\bullet-}$ based AOPs. It has been reported that AA can enhanced Fe(III)/PS system for contaminants degradation.[32] However, groundwater environment is typically anaerobic, which results in the precipitation of ferric iron to form minerals. Generally, iron exists mainly as dissolved Fe(II), AA could be enhance contaminants degradation in Fe(II)/PS system through regenerating Fe(III) to Fe(II) in theory, it is very necessary for us to systematically study AA enhanced ferrous/persulfate system for contaminants degradation.

Inspired by the previous findings on AA enhanced Fenton reaction and Fe(III)/PS system, AA-enhanced Fe(II)/PS system was initially investigated for contaminants degradation in this study. Tetracycline (TC) was selected as a model antibiotic contaminant to explore its degradation by AA-enhanced Fe(II)/PS system; the effects of Fe(II), PS, AA dosage and pH on TC degradation were investigated. It is expected to establish a new AOPs strategy for contaminated groundwater remediation.

2. Materials and methods

2.1 Reagents and materials

Potassium persulfate ($K_2S_2O_8$), ferrous sulfate heptahydrate ($FeSO_4 \cdot 7H_2O$), ascorbic acid ($C_6H_8O_6$), and tetracycline ($C_{22}H_{24}N_2O_8$) were purchased from Shanghai Titan Technology Co., Ltd. (Shanghai, China). 5,5-Dimethyl-1-pyrroline-*N*-oxide (DMPO) was provided by Sigma-Aldrich. Deionized (DI) water (18.2 MΩ cm) obtained from a Heal Force NW ultra-pure water system was used in all the experiments. All other chemicals were of above analytical grade.

2.2 Degradation experiments

The degradation of TC was carried out in a 250 mL glass vial. In a typical test, the vial was added by 173.8 mL of deionized water, 2 mL of 1 mM Fe(II), 3.2 mL of 50 mM PS, and 1 mL of 10 mM AA. Then, 20 mL of 100 mg L^{-1} TC was added to produce an initial concentration of 10 mg L^{-1}. The vial was stirred with a magnetic stirrer (25 °C) in darkness. At predetermined time intervals (0–60 min), 3 mL of mixed solution was taken for the analysis of TC concentrations. All experiments were carried out at least in duplicate.

2.3 Analysis

The absorbance of TC was detected by the UV-vis spectrophotometer (UV-5500, China) at a wavelength of 355 nm, and the concentration of TC was calculated through standard curve. The degradation of TC was calculated by eqn (1):

$$\text{Degradation (\%)} = 100(C_0 - C)/C_0 \quad (1)$$

The apparent rate constant k_{app1} and k_{app2} in the degradation process was obtain from the first-order and second-order models (eqn (2) and (3)) by linear regression respectively.

$$-\ln(C_t/C_0) = k_{app1}t \quad (2)$$

$$1/C_t - 1/C_0 = k_{app2}t \quad (3)$$

where C_0 is the initial concentration of TC and C is the concentration of TC at time t.

The formations of $SO_4^{\bullet-}$ and $^{\bullet}OH$ were identified by electron paramagnetic resonance (EPR, EMXplus-6/1, Bruker, Germany) with 5,5-dimethyl-1-pyrroline-*N*-oxide (DMPO) as the spin-trapping agent. The reaction solutions of PS (0.8 mM), Fe(II) (0.01 mM), AA (0.05 mM, in the Fe(II)/PS/AA system), and DMPO (100 mM) were mixed and reacted for 15 min and injected into a capillary tube for EPR test. The parameters of EPR spectrometer were set as follows: a center field of 3502 G, a microwave frequency of 9.85 GHz, a microwave power of 2.000 mW, a modulation frequency of 100 kHz, a modulation amplitude of 1.0 G.

Three-dimensional excitation–emission matrix fluorescence spectra (3D EEMs) were collected by using SmartFluo-pro spectrofluorimeter (Zolix, China) in the excitation wavelength range of λ_{ex} = 200–450 nm and in the emission wavelength range of λ_{em} = 300–500 nm.

3. Results and discussion

3.1 EPR studies

To explicitly identify the reactive oxidants for TC degradation, we tested the production of $SO_4^{\bullet-}$ and $^{\bullet}OH$ both in Fe(II)/PS and Fe(II)/PS/AA system. As shown in Fig. 1, there were both $SO_4^{\bullet-}$ and $^{\bullet}OH$ signals appeared in Fe(II)/PS and Fe(II)/PS/AA system. The spectrum of DMPO–OH adducts presented significant 1 : 2 : 2 : 1 signals,[33] whose signal intensity was much stronger than that of DMPO–SO_4 adducts presented a significant 1 : 1 : 1 : 1 : 1 : 1 signals.[34] This may be because DMPO–SO_4 is prone to hydrolysis in aqueous solution to produce DMPO–OH.[35] Hence, $^{\bullet}OH$ as the dominant radicals, was responsible for the TC degradation.

In order to confirm the enhancement of AA on the degradation of contaminants in the Fe(II)/PS system, we tested the production of $SO_4^{\bullet-}$ and $^{\bullet}OH$ both in Fe(II)/PS and Fe(II)/PS/AA system with different reaction time. As shown in Fig. 1a–d,

Open Access Article. Published on 09 November 2022. Downloaded on 7/28/2025 11:05:35 AM.
This article is licensed under a Creative Commons Attribution-NonCommercial 3.0 Unported Licence.

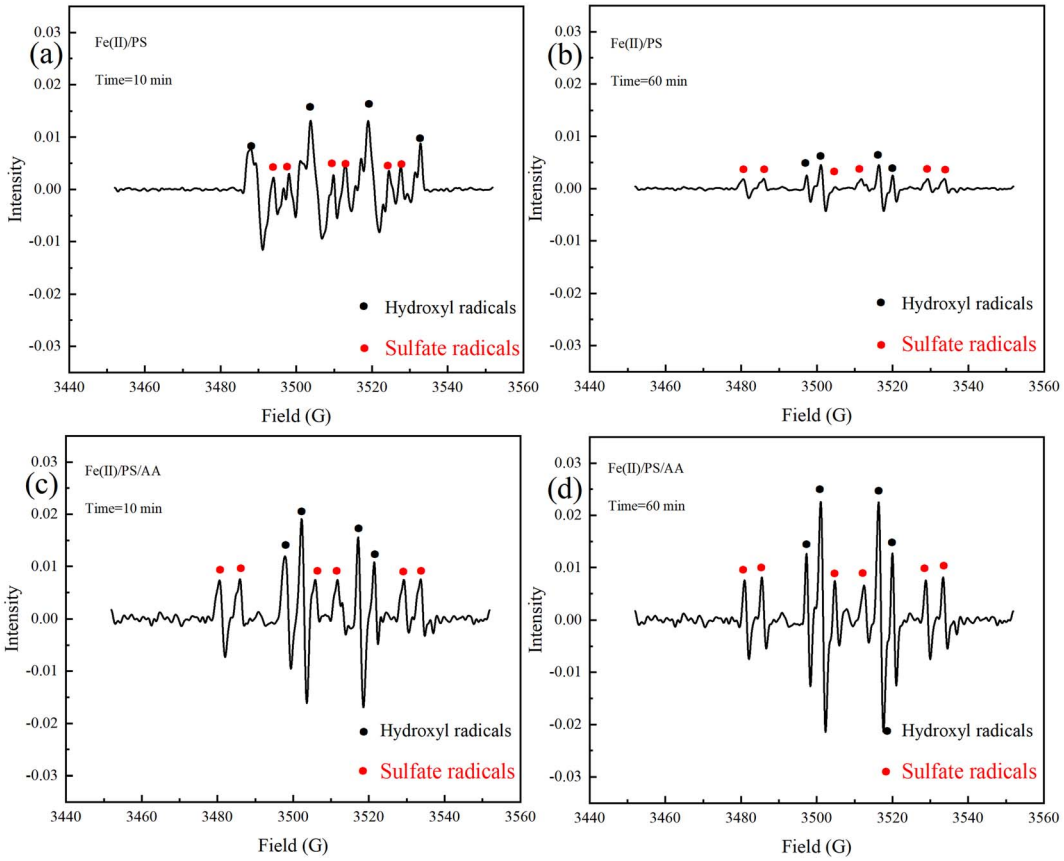


Fig. 1 EPR spectra of Fe(II)/persulfate system at the reaction time of (a) 10 min and (b) 60 min; EPR spectra of Fe(II)/persulfate/ascorbic acid system at the reaction time of (c) 10 min and (d) 60 min. Experimental conditions: persulfate (0.8 mM), Fe(II) (0.01 mM), ascorbic acid (0.05 mM, in the Fe(II)/persulfate/ascorbic acid system), and DMPO (100 mM) were mixed and reacted for 15 min.

the intensity of DMPO adducts signals in Fe(II)/AA/PS system was more stronger than that in Fe(II)/PS process, and the gap of the intensity of DMPO adducts signals in Fig. 1b and d (reaction for 60 min) was even higher than that of Fig. 1a and c (reaction for 10 min). In particular, the intensity of DMPO adducts signals in Fe(II)/AA/PS system has slightly increased (Fig. 1c and d), while the intensity of DMPO adducts signals in Fe(II)/PS system has gradually decreased as shown in Fig. 1a and b. The results revealed that the addition of AA could not only increase the concentrations of $SO_4^{\bullet-}$ and $^{\bullet}OH$ produced in Fe(II)/PS system, but also can continuously produce $SO_4^{\bullet-}$ and $^{\bullet}OH$ for contaminants degradation.

3.2 AA-enhanced Fe(II)/PS on the degradation of TC

To explore the effect of AA-enhanced Fe(II)/PS system on the degradation of TC, the other four systems, including PS, AA, Fe(II)/PS, and AA/PS, were used as comparisons. As shown in Fig. 2, it can be seen that AA and PS had hardly effect on the degradation of TC. When combining AA with PS, the degradation rate of TC by AA/PS system slightly increased to 18%. After adding Fe(II) in the PS system, Fe(II)/PS displayed an obvious improvement on the degradation effect of TC, and the degradation rate of TC reached to 72% when the reaction time was 60 min. This indicated that the addition of Fe(II) was beneficial for the reduction of PS to generate free radicals for the degradation of TC. Interestingly, the Fe(II)/PS/AA system could effectively remove TC and the degradation rate of TC increases to 86%, evidencing that Fe(II) can efficiently activate PS by AA facilitates the Fe(III)/Fe(II) cycle in the system, and then continuously generate free radicals to oxidize TC.

To clarify the kinetics of TC degradation in both Fe(II)/PS/AA and Fe(II)/PS systems, pseudo-first-order kinetic model and pseudo-second-order kinetic model were used to fit the experimental data, as shown in Fig. S1 and Table S1.† Compared with the pseudo-second-order kinetic model ($R^2 = 0.955$), the degradation kinetics in Fe(II)/PS/AA showed a better linear relationship with the pseudo-first-order kinetic model ($R^2 = 0.996$). For the Fe(II)/PS system, the experimental data of TC degradation is better fitted to the pseudo-first-order kinetic model ($R^2 = 0.994$) compared with pseudo-second-order kinetic model ($R^2 = 0.966$). Moreover, the apparent rate constant of TC from the pseudo-first-order kinetic model in the Fe(II)/PS system was found to be 0.0043 min^{-1}, which is much smaller than that of TC in the Fe(II)/PS/AA system (0.0266 min^{-1}). This result indicated that the addition of AA into the Fe(II)/PS system can significantly improve the degradation effect of TC.

3.3 Effect of Fe(II) dosage on the degradation of TC

The effect of Fe(II) dosage on the degradation of TC in the Fe(II)/PS/AA system was investigated in the range of 0.005–0.08 mM.

© 2022 The Author(s). Published by the Royal Society of Chemistry

Open Access Article. Published on 09 November 2022. Downloaded on 7/28/2025 11:05:35 AM.
This article is licensed under a Creative Commons Attribution-NonCommercial 3.0 Unported Licence.

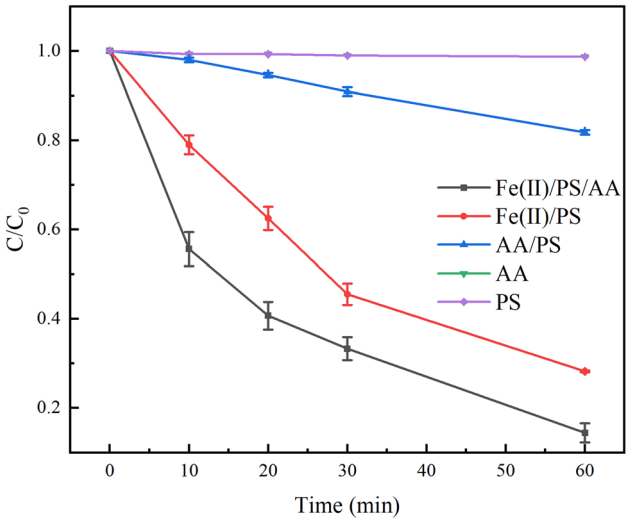


Fig. 2 Degradation of tetracycline in different reaction systems. Experimental conditions: (1) persulfate system: initially spiked tetracycline concentration = 10 mg L^{-1}, persulfate dosage = 0.8 mM; (2) ascorbic acid system: initially spiked tetracycline concentration = 10 mg L^{-1}, ascorbic acid dosage = 0.05 mM; (3) ascorbic acid/persulfate system: initially spiked tetracycline concentration = 10 mg L^{-1}, ascorbic acid dosage = 0.05 mM, persulfate dosage = 0.8 mM; (4) Fe(II)/persulfate system: initially spiked tetracycline concentration = 10 mg L^{-1}, Fe(II) dosage = 0.01 mM, persulfate dosage = 0.8 mM; (5) Fe(II)/persulfate/ascorbic acid system: initially spiked tetracycline concentration = 10 mg L^{-1}, Fe(II) dosage = 0.01 mM, persulfate dosage = 0.8 mM, ascorbic acid dosage = 0.05 mM, initial pH was not adjusted.

As shown in Fig. 3, when the Fe(II) dosage was less than 0.04 mM, the degradation rate of TC increased with increasing the Fe(II) dosage. The degradation rates of TC were 78%, 83%, and 85% when the Fe(II) dosage was 0.005, 0.01 and 0.02 mM respectively. However, an obvious decrease on the TC degradation rate was observed when the Fe(II) dosage exceeded 0.02 mM. For example, the Fe(II) dosage was 0.08 mM, the degradation rates of TC was only 70%. The results suggested that the excessive Fe(II) would quench the free radicals generated by activating PS to inhibit the degradation effect of TC (eqn (4))

$$SO_4^{\bullet -} + Fe(II) \rightarrow Fe(III) + SO_4^{2-}. \quad (4)$$

Interestingly, the degradation rate of TC with Fe(II) would be improved if the reaction time was extended, as shown in Fig. S2.† The degradation rate of TC with 0.005 mM of Fe(II) increases from 78% to 92% as the reaction time increases from 60 to 180 min. This indicated that the lower content of Fe(II) led to a lower reaction rate to generate free radicals, but continuous generation of free radicals can degrade contaminants completely by extending the reaction time.

From the above analysis, we can utilize the Fe(III)/Fe(II) cycling to continuously degradation TC by prolonging the reaction time under the low concentration of Fe(II) in the Fe(II)/PS/AA system. Therefore, we can construct a Fe(II)/PS/AA system by adding AA and PS for the remediation of contaminated groundwater, owing to the fact that a small concentration of Fe(II) generally exists in the actual groundwater.[36,37]

3.4 The effect of AA dosage on the degradation of TC

The effect of AA dosage on the degradation rate of TC in the Fe(II)/PS/AA system was shown in Fig. 4. The degradation rates of TC with 0.0125, 0.025, 0.05 and 0.1 mM of AA reached to 57%, 60%, 65% and 70% at the reaction time of 60 min, respectively. Clearly, the degradation rate of TC increases as the concentration of AA increases. Owing to the fact that the cycle rate of Fe(III)/Fe(II) increases with increasing the concentration of AA,

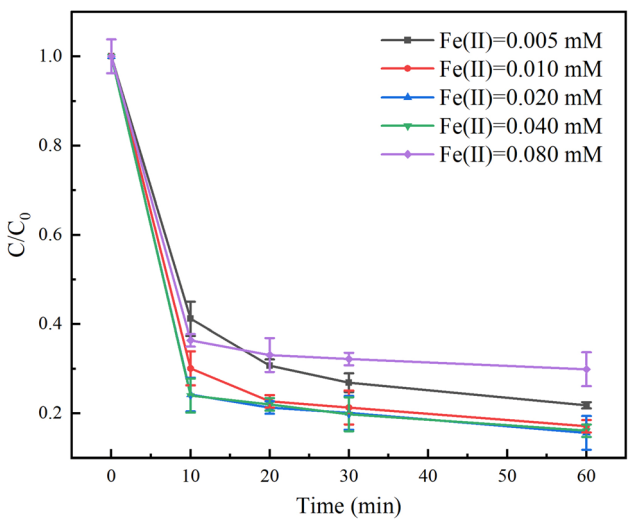


Fig. 3 Effect of Fe(II) dosage on degradation of tetracycline in Fe(II)/persulfate/ascorbic acid system. Experimental conditions: initially spiked tetracycline concentration = 10 mg L^{-1}, persulfate dosage = 0.8 mM, ascorbic acid dosage = 0.05 mM, initial pH was not adjusted.

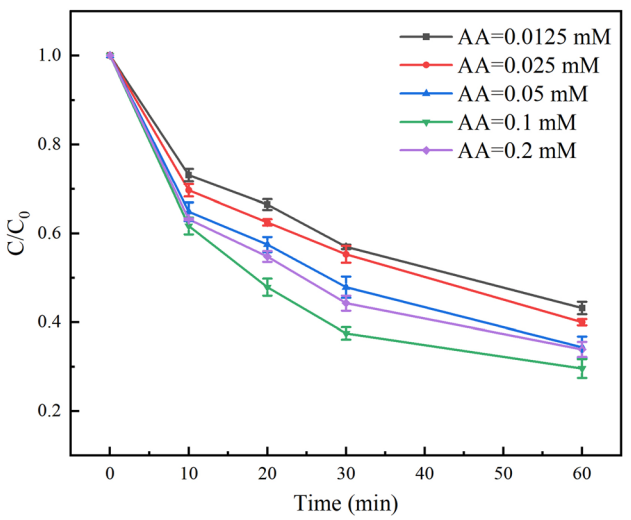


Fig. 4 Effect of ascorbic acid dosage on degradation of tetracycline in Fe(II)/persulfate/ascorbic acid system. Experimental conditions: initially spiked tetracycline concentration = 10 mg L^{-1}, Fe(II) dosage = 0.01 mM, persulfate dosage = 0.8 mM, initial pH was not adjusted.

Open Access Article. Published on 09 November 2022. Downloaded on 7/28/2025 11:05:35 AM.
This article is licensed under a Creative Commons Attribution-NonCommercial 3.0 Unported Licence.

Fe(II) can continuously activate PS to generate more free radicals for TC degradation. However, the degradation rate of TC decreases to 66% at the reaction time of 60 min when the dosage of AA is 0.2 mM, indicating that the excessive AA will compete with TC for consumption of free radicals. Therefore, when using AA to enhance Fe(II)/PS to remove contaminants, it is necessary to choose the suitable AA dosage, which can not only improve the removal effect of contaminants, but also effectively save the disposal cost.

3.5 Effect of PS dosage on the degradation of TC

The effect of PS dosage on the degradation of TC in the Fe(II)/PS/AA system was evaluated in the range of 0.10 and 1.60 mM. As shown in Fig. 5, the degradation rate of TC increased with increasing the PS dosage within 0.80 mM. The degradation rate of TC with 0.10 mM and 0.80 mM of PS were found to be 58% and 83% at the reaction time of 60 min, indicating that the increased PS is conducive to the Fe(II) activating PS to generate more free radicals for the TC degradation. However, when the PS dosage reached to 1.60 mM, the degradation rate of TC was reduced to 75%. Due to the excess of PS, PS will compete with TC and react with $SO_4^{\bullet -}$ radicals (eqn (5)), resulting in a inhibition in the degradation of TC.

$$SO_4^{\bullet -} + S_2O_8^{2-} \rightarrow SO_4^{2-} + S_2O_8^{\bullet -}. \quad (5)$$

Therefore, we should combine the contaminants degradation effect and economic cost factors to select the PS dosage in practical application of Fe(II)/PS/AA system.

3.6 The effect of pH on the degradation of TC

The pH for the degradation of TC in the Fe(II)/PS/AA solution was studied from 3 to 11. The pH was adjusted with 0.1 M H_2SO_4 and 0.1 M NaOH. The results in Fig. 6 showed that the degradation rates of TC by Fe(II)/PS/AA system decreased with increasing of pH. At the reaction time of 60 min, the degradation rates of TC reached to 77%, 73%, 69% when pH value was 3, 5, and 7, respectively, but the degradation rates of TC with 9 and 11 of pH were only 58% and 26%, respectively. The reason for these results might be that the formation of iron mineral colloids from Fe(III) under the alkaline condition, and the reduction rate of Fe(III) in the iron mineral colloids by AA is lower than that of Fe(III) under the homogeneous condition.[38] Based on the above speculation, the reaction time was extended, it was observed that TC can be completely degraded under alkaline condition of pH = 9 and 11 at the reaction time of 420 min and 660 min, respectively (Fig. S3†). Hence, these results revealed that Fe(II)/PS/AA system can effectively degrade contaminants over a wide pH range.

3.7 Recycling experiment

The good reusability of Fe(II) is beneficial to reduce the economic cost and avoid the formation of a large amount of iron sludge. We used the Fe(II) in the recycling system to degrade TC for evaluating the reusability of Fe(II). In three cycle experiments, a certain amount of TC, PS, and AA solutions were added to maintain the concentrations in a certain range before each cycle. As shown in Fig. 7a, the degradation rates of TC in three cycles were 86%, 76%, and 68%, respectively, indicating that Fe(II) exhibited good reusability for the degradation of TC in the Fe(II)/PS/AA. Moreover, the degradation kinetic of TC was studied, and the experiment data of three cycles is well conformed to pseudo-first-order kinetic model, as shown in Fig. S4a and Table S2.† Specifically, the apparent rate constants are 0.0308 min^{-1}, 0.0198 min^{-1}, and 0.0156 min^{-1}, respectively, and the corresponding half-lives are 22.5 min, 35.0 min, and 44.4 min. A large decrease in both degradation rate and

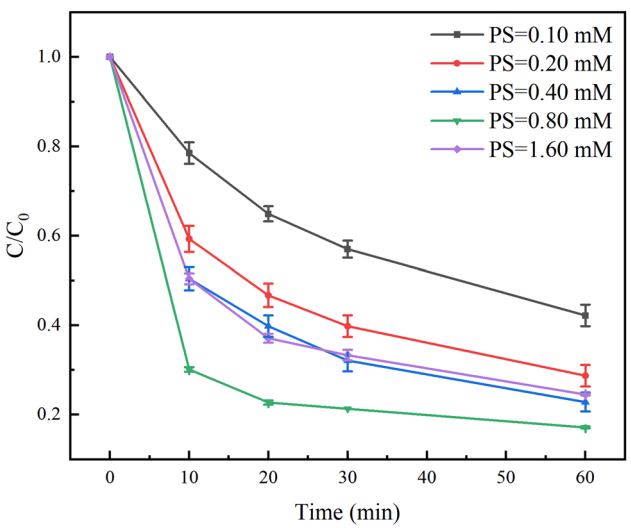


Fig. 5 Effect of persulfate dosage on degradation of tetracycline in Fe(II)/persulfate/ascorbic acid system. Experimental conditions: initially spiked tetracycline concentration = 10 mg L^{-1}, Fe(II) dosage = 0.01 mM, ascorbic acid dosage = 0.05 mM, initial pH was not adjusted.

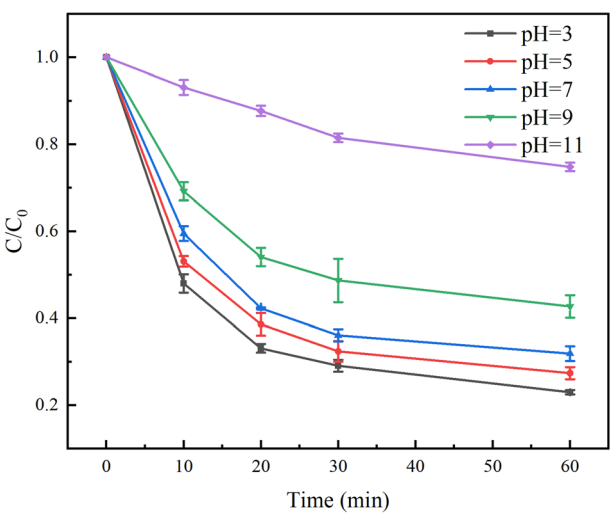


Fig. 6 Effect of pH on degradation of tetracycline in Fe(II)/persulfate/ascorbic acid system. Experimental conditions: initially spiked tetracycline concentration = 10 mg L^{-1}, Fe(II) dosage = 0.01 mM, persulfate dosage = 0.8 mM, ascorbic acid dosage = 0.05 mM.

© 2022 The Author(s). Published by the Royal Society of Chemistry

Open Access Article. Published on 09 November 2022. Downloaded on 7/28/2025 11:05:35 AM.
This article is licensed under a Creative Commons Attribution-NonCommercial 3.0 Unported Licence.

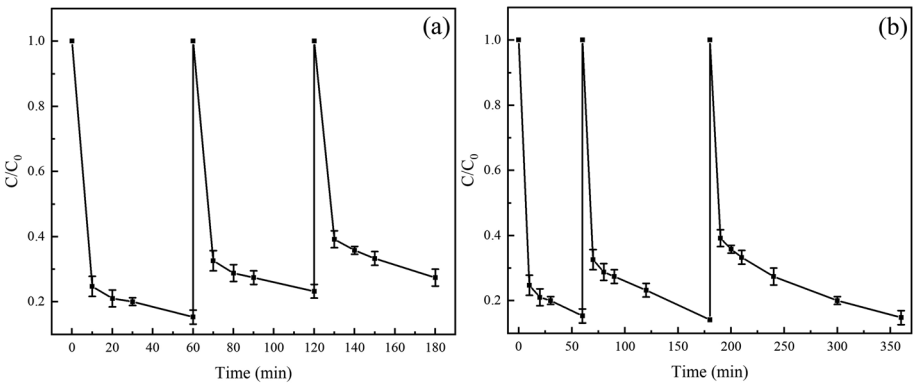


Fig. 7 Reusability of Fe(II) on degradation of tetracycline in Fe(II)/persulfate/ascorbic acid system. Experimental conditions: initially spiked tetracycline concentration = 10 mg L^{-1}, Fe(II) dosage = 0.01 mM, persulfate dosage = 0.8 mM, ascorbic acid dosage = 0.05 mM, initial pH was not adjusted.

apparent rate of TC is observed, probably due to the decrease of Fe(II) activity and the decreasing reduction rate of PS by Fe(II) during the recycling processes. On the basis of the good ability of AA to facilitate the Fe(III)/Fe(II) cycle, it is speculated that the Fe(II) in the Fe(II)/PS/AA system can still completely remove TC by prolonging the reaction time after multiple cycles.

To verify the above speculation, we set up another set of experiments with three cycles. During the experiment, after the end of the previous cycle with TC complete degradation, added a certain amount of TC, PS and AA solutions to restore the concentration of TC, PS and AA to the initial concentration, and then started the next cycle. The results show that TC can be completely removed in three cycles, and the time of TC degradation required is 60, 180 and 240 min, respectively. The degradation process of TC in the three cycles all fitted to the pseudo first-order kinetic model. The apparent rate constants are 0.0303, 0.0153, and 0.0111 min^{-1}, respectively, and the corresponding half-lives are 22.9, 45.3, and 62.4 min, respectively. The change trend is consistent with the results obtained in Fig. 7a.

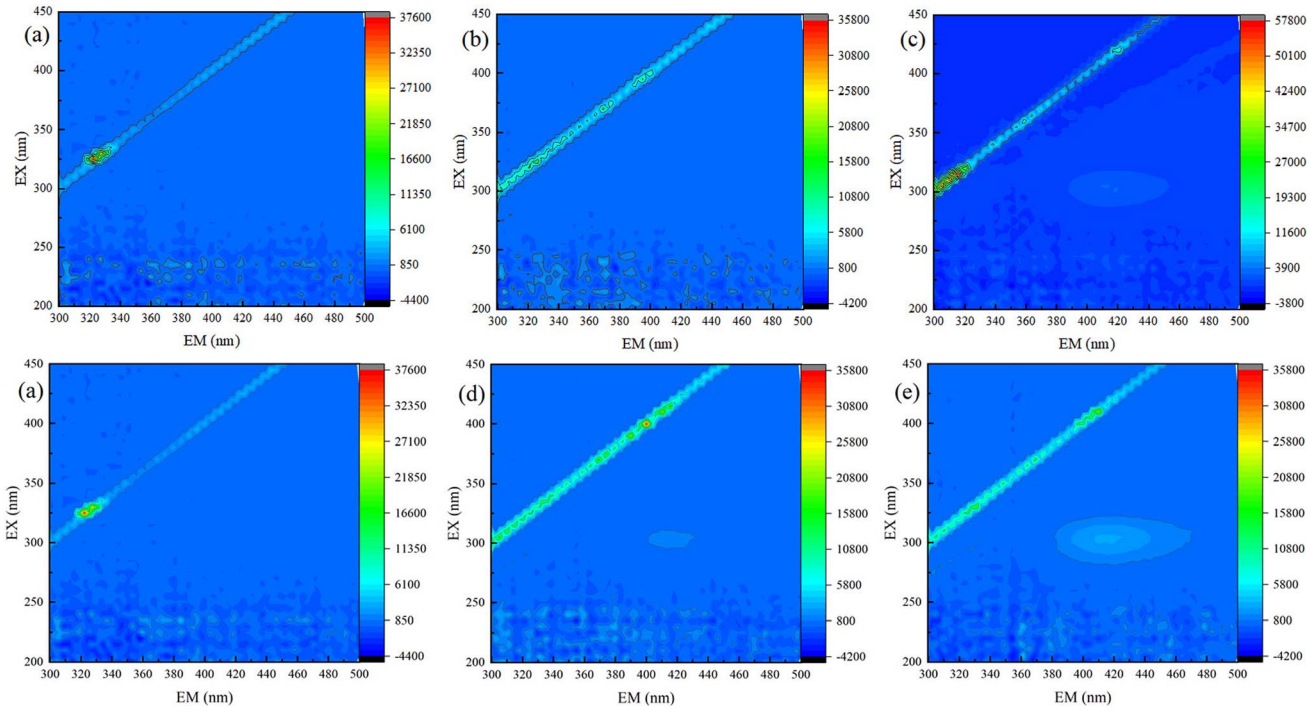


Fig. 8 3D EEMs of tetracycline before and after degradation. (a) 3D EEMs of tetracycline before the beginning of tetracycline degradation (M1); 3D EEMs of tetracycline in Fe(II)/persulfate system at the reaction time of (b) 10 min (M2) and (c) 60 min (M3); 3D EEMs of tetracycline in Fe(II)/persulfate/ascorbic acid system at the reaction time of (d) 10 min (M4) and (e) 60 min (M5). Experimental conditions: initially spiked tetracycline concentration = 10 mg L^{-1}, persulfate (0.8 mM), Fe(II) (0.01 mM), ascorbic acid (0.05 mM, in the Fe(II)/persulfate/ascorbic acid system), initial pH was not adjusted.

© 2022 The Author(s). Published by the Royal Society of Chemistry

Open Access Article. Published on 09 November 2022. Downloaded on 7/28/2025 11:05:35 AM.
This article is licensed under a Creative Commons Attribution-NonCommercial 3.0 Unported Licence.

The application of Fe(II)/PS/AA in industrial wastewater treatment might be limited from the results in Fig. 7a, because of the shorter residence time. On the other hand, considering the conditions for the reuse of Fe(II), Fe(II)/PS/AA can completely degrade TC by giving enough reaction time. Thus, Fe(II)/PS/AA can be applied to the remediation of groundwater contaminants (Fig. 7b), owing to the fact that groundwater environments contain a trace of Fe(II) and *in situ* remediation is usually used.

3.8 Three dimensional fluorescence spectrum analysis

In order to confirm that TC has been degraded, solution samples of different reaction processes were characterized by 3D EEMs. As shown in Fig. 8a, no fluorescence peak could be observed before the beginning of TC degradation process (M1), this is because TC can quench fluorescence.[39] As shown in Fig. 8, Except of sample M2 (Fig. 8b), there was all one fluorescence peak ($\lambda_{ex}/\lambda_{em}$ = (250–400 nm)/(380–500 nm)) appeared in the samples of M3, M4, and M5 (Fig. 8c–e), which was represented humic acids-like substances.[40,41] The peak area increased with reaction proceeding, which indicated that TC has been effectively degraded both in Fe(II)/PS system and Fe(II)/PS/AA system.

Especially, comparing Fig. 8b (M2) with Fig. 8d (M4), it was that the peak area was much larger in Fe(II)/PS/AA system than that of in Fe(II)/PS system. The similar trend was observed in samples of M3 (Fig. 8c) and M5 (Fig. 8e). That was same as the results shown in Fig. 8c (M3) and Fig. 8e (M5). It revealed that AA can efficiently enhance Fe(II)/PS system for TC degradation.

4. Conclusion

In this paper, AA-enhanced Fe(II)/PS system was developed for the degradation of TC. Both $SO_4^{\bullet-}$ and $^{\bullet}OH$ play important roles for contaminants degradation in the Fe(II)/PS/AA process, whereas the dominant oxidant species is $^{\bullet}OH$, instead of $SO_4^{\bullet-}$. Several parameters were investigated for optimizing the dosage of system components, including Fe(II), AA, PS dosage and pH value. The degradation of Fe(II)/PS/AA system for TC was better than those of PS, AA, Fe(II)/PS, and AA/PS system. Appropriate Fe(II), AA, PS dosage can effectively improve the degradation effect of TC. Additionally, the degradation rate of TC in the Fe(II)/PS/AA system under acidic condition is higher than that of under alkaline condition. With the increase of reaction time, TC can also be completely degraded under alkaline condition or with little ferrous in Fe(II)/PS/AA system. Furthermore, the recycling experiment of Fe(II)/PS/AA system showed that Fe(II) exhibited good reusability. More importantly, benefiting from the less Fe(II) dosage and a wide pH range advantages, Fe(II)/PS/AA system can be widely used in the remediation of actual contaminated groundwater.

Conflicts of interest

The authors declare no conflict of interest.

Acknowledgements

This work was supported by the Natural Science Foundation of China (Grant No. 41967030), Guangxi Natural Science Foundation (Grant No. 2020GXNSFAA159170), and the Young Scholar Innovation Team of Guangxi Minzu University (2022).

References

1 Q. Q. Zhang, G. G. Ying, C. G. Pan, Y. S. Liu and J. L. Zhao, Comprehensive evaluation of antibiotics emission and fate in the river basins of China: Source analysis, multimedia modelling, and linkage to bacterial resistance, *Environ. Sci. Technol.*, 2015, **49**, 6772–6782.

2 C. X. Yan, Y. Yang, J. L. Zhou, M. Liu, M. H. Nie, H. Shi and L. J. Gu, Antibiotics in the surface water of the Yangtze Estuary: Occurrence distribution and risk assessment, *Environ. Pollut.*, 2013, **175**, 22–29.

3 Z. Pan, S. D. Yang, L. X. Zhao, X. J. Li, L. P. Weng, Y. Sun and Y. T. Li, Temporal and spatial variability of antibiotics in agricultural soils from Huang-Huai-Hai Plain, northern China, *Chemosphere*, 2021, **272**, 129803.

4 R. Zuo, X. Liu, Q. R. Zhang, J. S. Wang, J. Yang, Y. G. Teng, X. J. Chen and Y. Z. Zhai, Sulfonamide antibiotics in groundwater and their migration in the vadose zone: A case in a drinking water resource, *Ecol. Eng.*, 2021, **162**, 106175.

5 Y. P. Ma, M. Li, M. M. Wu, Z. Li and X. Liu, Occurrences and regional distributions of 20 antibiotics in water bodies during groundwater recharge, *Sci. Total Environ.*, 2015, **518–519**, 498–506.

6 R. López-Serna, A. Jurado, E. Vázquez-Suñé, J. Carrera, M. Petrović and D. Barceló, Occurrence of 95 pharmaceuticals and transformation products in urban groundwaters underlying the metropolis of Barcelona, Spain, *Environ. Pollut.*, 2013, **174**, 305–315.

7 Y. Feng, D. L. Wu, H. L. Li, J. F. Bai, Y. B. Hu, C. Z. Liao, X. Y. Li and K. M. Shih, Activation of persulfates using siderite as a source of ferrous ions: Sulfate radical production, stoichiometric efficiency, and implications, *ACS Sustainable Chem. Eng.*, 2018, **6**(3), 3624–3631.

8 G. P. Anipsitakis and D. D. Dionysiou, Degradation of organic contaminants in water with sulfate radicals generated by the conjunction of peroxymonosulfate with cobalt, *Environ. Sci. Technol.*, 2003, **37**(20), 4790–4797.

9 A. Tsitonaki, B. Petri, M. Crimi, H. Mosbk, R. L. Siegrist and P. L. Bjerg, In situ chemical oxidation of contaminated soil and groundwater using persulfate: A review, *Crit. Rev. Environ. Sci. Technol.*, 2010, **40**(1), 55–91.

10 L. W. Matzek and K. E. Carter, Activated persulfate for organic chemical degradation: A review, *Chemosphere*, 2016, **151**, 178–188.

11 X. Lu, Y. S. Shao, N. Y. Gao, J. X. Chen, Y. S. Zhang, H. M. Xiang and Y. L. Guo, Degradation of diclofenac by UV-activated persulfate process: Kinetic studies, degradation pathways and toxicity assessments, *Ecotoxicol. Environ. Saf.*, 2017, **141**, 139–147.

© 2022 The Author(s). Published by the Royal Society of Chemistry

Open Access Article. Published on 09 November 2022. Downloaded on 7/28/2025 11:05:35 AM.
This article is licensed under a Creative Commons Attribution-NonCommercial 3.0 Unported Licence.

12 I. A. Ike, J. D. Orbell and M. Duke, Activation of Persulfate at Waste Heat Temperatures for Humic Acid Degradation, *ACS Sustainable Chem. Eng.*, 2018, **6**, 4345–4353.

13 C. M. Dominguez, V. Rodriguez, E. Montero, A. Romero and A. Santos, Abatement of dichloromethane using persulfate activated by alkali: A kinetic study, *Sep. Purif. Technol.*, 2020, **241**, 116679.

14 J. Zhu, Y. N. Song, L. W. Wang, Z. R. Zhang, J. Gao, D. C. W. Tsang, Y. S. Ok and D. Y. Hou, Green remediation of benzene contaminated groundwater using persulfate activated by biochar composite loaded with iron sulfide minerals, *Chem. Eng. J.*, 2022, **429**, 132292.

15 C. Q. Wang, R. Huang, R. R. Sun, J. P. Yang and M. Sillanpää, A review on persulfates activation by functional biochar for organic contaminants removal: synthesis, characterizations, radical determination, and mechanism, *J. Environ. Chem. Eng.*, 2021, **9**, 106267.

16 X. W. Chen, B. Yang, P. Oleszczuk, Y. Z. Gao, X. J. Yuan, W. T. Ling and M. G. Waigi, Vanadium oxide activates persulfate for degradation of polycyclic aromatic hydrocarbons in aqueous system, *Chem. Eng. J.*, 2019, **364**, 79–88.

17 I. Hussain, Y. Zhang and S. Huang, Degradation of aniline with zero-valent iron as an activator of persulfate in aqueous solution, *RSC Adv.*, 2014, **4**, 3502–3511.

18 P. Zhou, J. Zhang, J. Liang, Y. Zhang, Y. Liu and B. Liu, Activation of persulfate/copper by hydroxylamine via accelerating the cupric/cuprous redox couple, *Water Sci. Technol.*, 2016, **73**(3), 493–500.

19 X. R. Xu and X. Z. Li, Degradation of azo dye Orange G in aqueous solutions by persulfate with ferrous ion, *Sep. Purif. Technol.*, 2010, **72**(1), 105–111.

20 X. Wu, X. Gu, S. Lu, M. Xu, X. Zang, Z. Miao, Z. Qiu and S. Qian, Degradation of trichloroethylene in aqueous solution by persulfate activated with citric acid chelated ferrous ion, *Chem. Eng. J.*, 2014, **255**, 585–592.

21 S. H. Yuan, P. Liao and A. N. Alshawabkeh, Electrolytic manipulation of persulfate reactivity by iron electrodes for trichloroethylene degradation in groundwater, *Environ. Sci. Technol.*, 2014, **48**(1), 656–663.

22 Z. Yan, Y. Gu, X. Wang, Y. Hu and X. Li, Degradation of aniline by ferrous ions activated persulfate: Impacts, mechanisms, and by-products, *Chemosphere*, 2021, **268**, 129237.

23 A. Rastogi, S. R. Al-Abed and D. D. Dionysiou, Effect of inorganic, synthetic and naturally occurring chelating agents on Fe(II) mediated advanced oxidation of chlorophenols, *Water Res.*, 2009, **43**, 684–694.

24 X. L. Wu, X. G. Gu, S. G. Lu, M. H. Xu, X. K. Zang, Z. W. Miao, Z. F. Qiu and Q. Sui, Degradation of trichloroethylene in aqueous solution by persulfate activated with citric acid chelated ferrous ion, *Chem. Eng. J.*, 2014, **255**, 585–592.

25 Q. L. Ma, H. X. Zhang, X. Y. Zhang, B. Li, R. N. Guo, Q. F. Cheng and X. W. Cheng, Synthesis of magnetic CuO/$MnFe2O_4$ nanocompisite and its high activity for degradation of levofloxacin by activation of persulfate, *Chem. Eng. J.*, 2019, **360**, 848–860.

26 Z. Y. Li, L. Wang, Y. L. Liu, Q. Zhao and J. Ma, Unraveling the interaction of hydroxylamine and Fe(III) in Fe(II)/Persulfate system: A kinetic and simulating study, *Water Res.*, 2020, **168**, 115093.

27 L. Davidsson, P. Galan, P. Kastenmayer, F. Cherouvrier, M. A. Juillerat, S. Hercberg and R. F. Hurrell, Iron bioavailability studied in infants: the influence of phytic acid and ascorbic acid in infant formulas based on soy isolate, *Pediatr. Res.*, 1994, **36**, 816–822.

28 Z. M. Wang, W. D. C. Schenkeveld, S. M. Kraemer and D. E. Giammar, Synergistic Effect of Reductive and Ligand Promoted Dissolution of Goethite, *Environ. Sci. Technol.*, 2015, **49**, 7236–7244.

29 O. Larsen and D. Postma, Kinetics of reductive bulk dissolution of lepidocrocite, ferrihydrite, and goethite, *Geochem. Cosmochim. Acta*, 2001, **65**, 1367–1379.

30 M. D. S. Afonso, P. J. Morando, M. A. Blesa, S. Banwart and W. Stumm, The reductive dissolution of iron oxides by ascorbate: The role of carboxylate anions in accelerating reductive dissolution, *J. Colloid Interface Sci.*, 1990, **138**, 74–82.

31 X. J. Hou, X. P. Huang, M. L. Li, Y. S. Zhang, S. H. Yuan, Z. H. Ai, J. C. Zhao and L. Z. Zhang, Fenton oxidation of organic contaminants with aquifer sediment activated by ascorbic acid, *Chem. Eng. J.*, 2018, **348**, 255–262.

32 L. Yang, H. Zhang, J. W. Wang and J. Ai, Rapid and continuous oxidation of organic contaminants with ascorbic acid and a modified ferric/persulfate system, *Chem. Eng. J.*, 2015, **270**, 73–79.

33 X. D. Shi, Y. T. Li, Z. Zhang, L. Sun and Y. Z. Peng, Enhancement of ciprofloxacin degradation in the Fe(II)/peroxymonosulfate system by protocatechuic acid over a wide initial pH range, *Chem. Eng. J.*, 2019, **372**, 1113–1121.

34 C. Y. Zhu, G. D. Fang, D. D. Dionysiou, C. Liu, J. Gao, W. X. Qin and D. M. Zhou, Efficient transformation of DDTs with persulfate activation by zero-valent iron Nanoparticles: A mechanistic study, *J. Hazard. Mater.*, 2016, **316**, 232–241.

35 G. S. Timmins, K. J. Liu, E. J. H. Bechara, Y. Kotake and H. M. swartz, Trapping of free radicals with direct in vivo EPR detection: a comparison of 5,5-dimethyl-1-pyrroline-N-oxide and 5-diethoxyphosphoryl-5-methyl-1-pyrroline-N-oxide as spin traps for HO· and $SO4^{\cdot-}$, *Free Radical Biol. Med.*, 1999, **27**(3/4), 329–333.

36 C. D. Johnson, A. Nandi, T. A. Joyner and I. Luffman, Iron and manganese ingroundwater: using Kriging and GIS to locate high concentrations in Buncombe County, North Carolina, *Groundwater*, 2018, **56**(1), 87–95.

37 Z. Zhang, C. Xiao, O. Adeyeye, W. Yang and X. Liang, Source and mobilization mechanism of iron, manganese and arsenic in groundwater of Shuangliao City, Northeast China, *Water*, 2020, **12**, 534.

38 Y. T. Lin, C. J. Liang and C. W. Yu, Trichloroethylene Degradation by Various Forms of Iron Activated Persulfate Oxidation with or without the Assistance of Ascorbic Acid, *Ind. Eng. Chem. Res.*, 2016, **55**(8), 2302–2308.

Open Access Article. Published on 09 November 2022. Downloaded on 7/28/2025 11:05:35 AM.
This article is licensed under a Creative Commons Attribution-NonCommercial 3.0 Unported Licence.



39 Y. J. Shi, S. F. Xing, X. H. Wang and S. G. Wang, Changes of the reactor performance and the properties of granular sludge under tetracycline (TC) stress, *Bioresour. Technol.*, 2013, **139**, 170–175.

40 W. Chen, P. Westerhoff, J. A. Leenheer and K. Booksh, Fluorescence excitation-emission matrix regional integration to quantify spectra for dissolved organic matter, *Environ. Sci. Technol.*, 2003, **37**(24), 5701–5710.

41 H. Wang, X. Z. Yuan, Y. Wu, G. M. Zeng, H. R. Dong, X. H. Chen, L. J. Leng, Z. B. Wu and L. J. Peng, In situ synthesis of In_2S3@MIL-125(Ti) core–shell microparticle for the removal of tetracycline from wastewater by integrated adsorption and visible-light-driven photocatalysis, *Appl. Catal., B*, 2016, **186**, 19–29.

© 2022 The Author(s). Published by the Royal Society of Chemistry